GRADIVA

Volume 63 | Issue 02 | February 2024
DOI: 10.5281/zenodo.10682775

Wear Model of The TPU 16 03 08 H10F Cutting Insert in Orthogonal Cutting

Leila Zouambi [1,2]*, Mokhtar Bourdim [3] & Siham Kerrouz [1,4]

1. Mechanical Engineering Department, University of Relizane, 48000, Algeria.
2. Mechanical Physical Materials Laboratory (LMPM),
Mechanical Engineering Department, University of Sidi Bel-Abbes 22000, Algeria.
*Corresponding Author Email: leila.zouambi@univ-relizane.dz, ORCID ID: https://orcid.org/ 0000-0002-1732-5237
3. Mechanical Engineering Department, University Center of Maghnia, Tlemcen, Algeria.
4. Laboratory of Gaseous Fuel and Environment (LCGE), University Mohamed Boudiaf, Oran, Algeria.

Abstract

The consequences induced by the cut, in terms of residual stresses, strongly depend on the operating conditions and the evolution of the wear of the cutting tools. This wear is indeed a complex phenomenon to study due to the multitude of its origins, in particular physico-chemical (affinities between certain constituent materials of the plate/part pair, etc.) or thermo-mechanical (abrasion, diffusion, adhesion, etc.).). Also, the wear of the cutting tools has a considerable impact on the course of the cutting operation: increased cutting forces, vibrations, etc. In our work, the main goal is to develop a finite element cutting model, using the ABAQUS© calculation code, to simulate the wear of cutting tools. We are interested in the case of the orthogonal cut of low alloy steel 42CrMo4, widely used in the industrial environment, and this by an uncoated tungsten carbide tool.

Keywords: *Residual Stresses, Cutting Tools, Thermo-Mechanical Cutting Operation, Cutting Forces, Orthogonal Cut, Tungsten Carbide Tool.*

1. INTRODUCTION

Although cutting tool machining is one of the most widespread material removal processes, modelling this phenomenon is far from trivial. It is particularly complex due to the diversity of the physical phenomena involved, in particular the presence of large elastoplastic deformations [1], the complexity of contact and friction characterizing the tool-material interaction [2, 3], the thermo-mechanical coupling of the process and the diversity of mechanisms during chip formation [4-10]. Also, the wear of the cutting tools has a considerable impact on the course of the cutting operation [11-16]: increased cutting forces [17], vibrations [18], etc.

The chip separation follows a line of separation but which is not determined beforehand [19-23]. The formation of the chip is modelled either by crack propagation in 2D [24], or by removal of elements in 2D and 3D [25].

In the field of mechanical manufacturing, the phenomenon of wear is perceived as a major problem to be solved [26,27]. It is therefore essential to understand the mechanisms that govern this wear. According to Shaw [28], three modes of wear can be listed: abrasive wear, adhesive wear and diffusion wear.

Khrais et al [29] observed wear caused by machining 42CrMo4 steel with a coated cemented carbide tool. Figure 9 illustrates SEM images of wear observed on the flank face for a cutting speed of 360 m/min, a feed rate of 0.14 mm/rev and a depth of cut of 1 mm.

Volume 63 | Issue 02 | February 2024
DOI: 10.5281/zenodo.10682775

The simulated machining time is a key point for estimating the wear of a given insert, under specific cutting conditions. Indeed, wear appears experimentally after a few seconds, while most numerical simulations are a few milliseconds under orthogonal (2D) cutting conditions while requiring several CPU hours of calculation [30-33].

This article is dedicated to the experimental study carried out as part of our work and which aims to analyze the influence of machining conditions (cutting speed, feed, etc.) on the phenomenon of wear of cutting inserts in turning and also to see the evolution of this phenomenon over time. This study will also make it possible to improve and validate the numerical model developed.

All the tests were carried out according to an orthogonal cutting configuration for machining 42CrMo4 steel, a material frequently used in the industrial environment. Machining is done with an uncoated tungsten carbide insert. The experimental device deployed within the framework of this study is presented, namely the materials studied and the experimental means implemented (machines, measuring devices, etc.) [34].

The presentation of the test protocol and in particular of the preliminary test campaign which was conducted to be within a range of cutting speeds conducive to the observation of the phenomenon of wear with reasonable machining times are submitted. Having chosen the cutting conditions to be varied, 36 trials with a different torque (V_c, f) were carried out at machining times ranging from 10 to 40 seconds.

The effect of variation in cutting conditions on the machining of 42CrMo4 steel has been the subject of several studies. Machining 42CrMo4 steel, known for its high hardness, presents challenges due to its material properties [35-38]. Furthermore, research has been conducted on the influence of flank wear on forces in orthogonal turning of 42CrMo4 steel, evaluating the capacity of finite element analysis in understanding the effect of flank wear evolution on machining forces 5. These studies collectively demonstrate the significance of cutting conditions on the machining of 42CrMo4 steel, particularly in relation to cutting force components, surface roughness, and the influence of flank wear.

The morphology of the chip is also part of this study. The chips collected following each machining operation were analyzed in order to determine the effect of the variation of the cutting conditions on the machining of 42CrMo4 steel. During these experimental tests, the evolutions of the wear on the rake face and the relief face and this by 3D microscopy were also analyzed. The influence of each parameter cutting (V_c and f) is evaluated on the evolution of wear. The main results from the test campaign are presented.

2. EXPERIMENTAL DEVICE

The material studied is 42CrMo4. It is a low strength steel alloyed with chromium and molybdenum, which offers a good compromise between hardness and resilience in the quenched and tempered state. This material also has good wear resistance. This steel is frequently used in the industrial sector with very varied fields of application, in particular for the production of shafts, gears and mechanical parts working to wear. This material is delivered in the form of bars as part of this study by the manufacturer COUZON ACIERS SERVICE. The chemical composition of the batch studied is presented in Table 1.

Volume 63 | Issue 02 | February 2024
DOI: 10.5281/zenodo.10682775

Table 1: Designation of 42CrMo4 steel according to the standard.

Elements	C	Si	Mn	S	P	Cr	Mo	Ni
%	0,41	0,27	0,82	0,028	0,015	1,02	0,198	0,05

The cutting tool used in this study is a cutting insert from the manufacturer SANDVICK COROMONT. This is an uncoated triangular insert reference TPUN 16 03 08 H10F with tungsten carbide (WC) as substrate is shown in Figure 1.

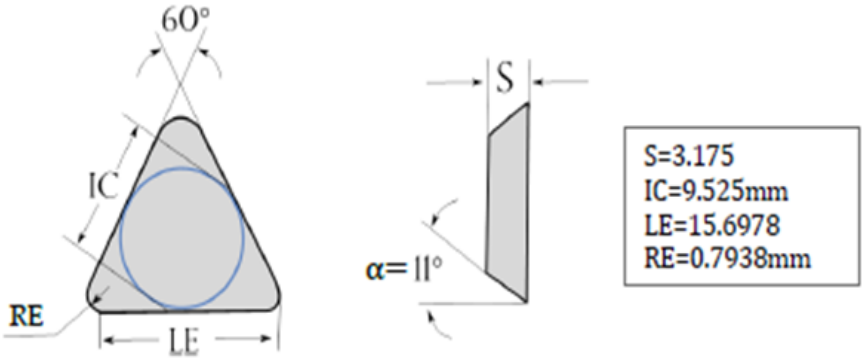

Figure 1: Geometric characteristics of the TPN 16 03 08 H10F insert [Sandvik].

With:

IC: diameter of the inscribed circle

LE: Effective cutting edge length

RE: Nose radius

S: Insert thickness

The machining was carried out on a TOS model SN40C universal lathe from the technological hall of the University Abou Bekr Blkaid Tlemcen Algeria, whose electric motor power is 6.8 kW. The latter is equipped with a spindle whose rotation frequency can reach 3500 rpm with a maximum power of 30 Kw Figure 2. Given that the material to be studied is in the form of 42CrMo4 bars 500 mm long and 200 mm in diameter and that the tests will be carried out on discs 3 mm thick, it was decided to make grooves on these cylinders so as to obtain discs, the machining is done without lubrication.

Figure 2: General view of machining.

Volume 63 | Issue 02 | February 2024
DOI: 10.5281/zenodo.10682775

The wear measurement on the pads is done using an ALICONA® Infinite Focus 3D surface measurement system given in Figure 3, which provides both shape and roughness measurement by optical method with a high resolution of up to at 20 nm. The operating principle of this system is to combine an optical microscope and a camera. It uses a color contrast sensor and makes it possible, from the variation of focus, to generate topographic information combined with a color image. An accurate 3D measurement is given by the software from this information. On the other hand, the force measurements are carried out using a KISTLER type 9257A dynamometer.

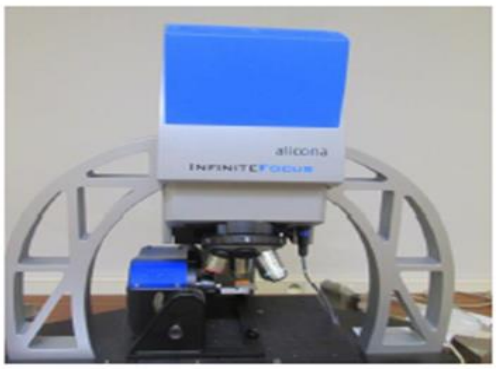

Figure 3: ALICONA surface measuring equipment.

The observation of crater wear on the turning inserts is done using the 3D microscopy measurement system: ALICONA®. To measure the characteristic quantities of wear, both on the rake face and on the clearance face, a special set-up was designed Figure 4 (c). This saves considerable time by automatically turning the insert, which avoids its manual repositioning. The measurement system allows the reconstruction of the cutting edge: cutting face, clearance face and the junction between the 2 Figure 4 (b). Figure 4 (d) shows the various parameters to be measured on the wafer.

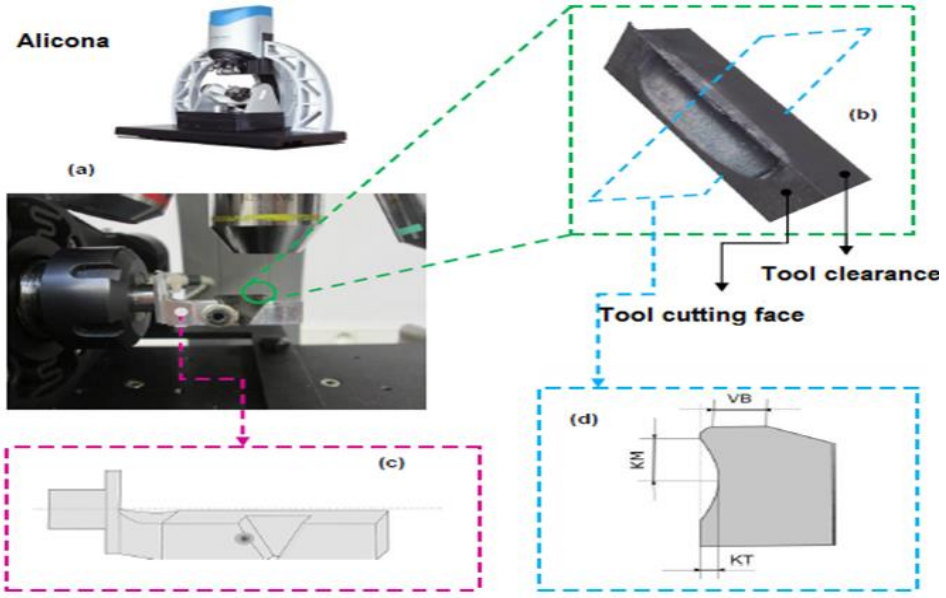

Figure 4: Measurement of wear parameters via ALICONA: (a). Experimental device (b). Reconstruction of the leading and clearance faces (c). Special assembly for wear measurement (d). Wear parameters to be measured.

Volume 63 | Issue 02 | February 2024
DOI: 10.5281/zenodo.10682775

The cutting parameters to be adopted for the wear tests are presented by the diagram in Figure 5. The choice for the cutting speeds will be limited to only 3 values so as not to have a very high number of trials. Thus, the cutting speeds chosen for this study are V_c=120, 150 and 180m/min.

The selected feeds are f=0.1, 0.15 and 0.2 mm/rev. For each couple (V_c, f) indicated in Figure 5 by a number (from 1 to 9), a series of tests is carried out at different machining times: T_u = [10s, 20s, 30s, 40s].

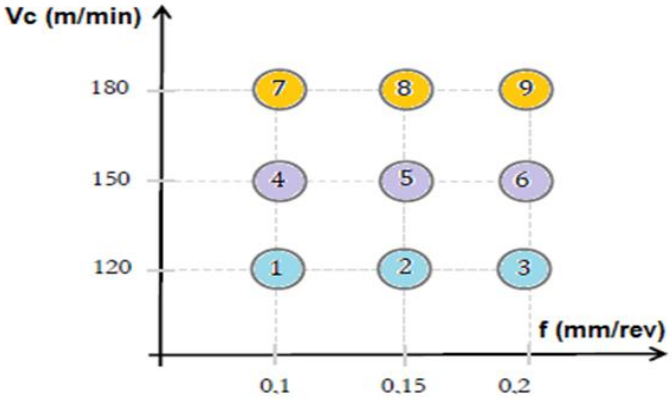

Figure 5: Cutting parameters chosen for wear tests.

3. RESULTS AND DISCUSSIONS

On the rake face, the wear parameters KM and KT are measured on the considered insert as shown in the Figure 6.

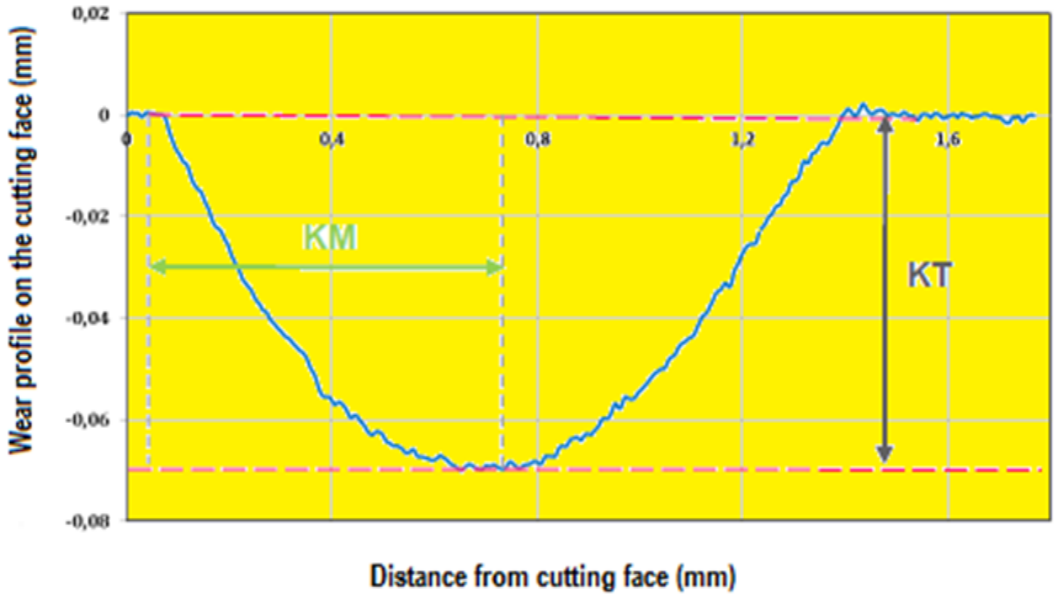

Figure 6: Crater wear profile: V_c = 180m/min; f = 0.2mm/rev; a_p = 3mm; T_u = 40s.

For each of the combinations of the tests (V_c, f), the wear on the rake face of the tool was measured via ALICONA. Figure 7 illustrates the evolution of crater wear over time (10s, 20s, 30s, 40s) for the following cutting conditions: V_c=180m/min, f=0.2mm/rev and a_p=3mm.

Volume 63 | Issue 02 | February 2024
DOI: 10.5281/zenodo.10682775

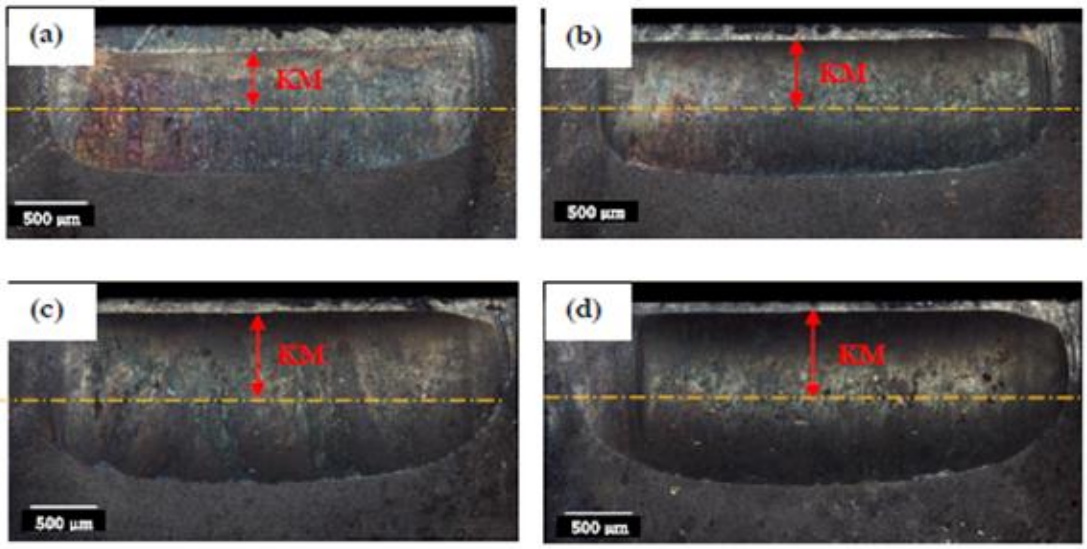

Figure 7: Evolution of crater wear over time at V_c = 180m/min, f = 0.2mm/rev and a_p = 3mm (a). T_u = 10s; (b). T_u = 20s; (vs). T_u = 30s; (d). T_u = 40s.

In order to better understand the wear of the tool and to establish a law of wear (in particular the law of Preston-Archard) [39], the volume of the worn surface on the cutting face of the tool is measured through ALICONA.

The measurements also make it possible to see the evolution of the wear profile on the cutting face of the tool over time. By way of example, Figure 8 illustrates the evolution of this profile at different machining times: 10s, 20s, 30s and 40s and this for the following cutting conditions: V_c=150m/min; f=0.2mm/rev; a_p=3mm.

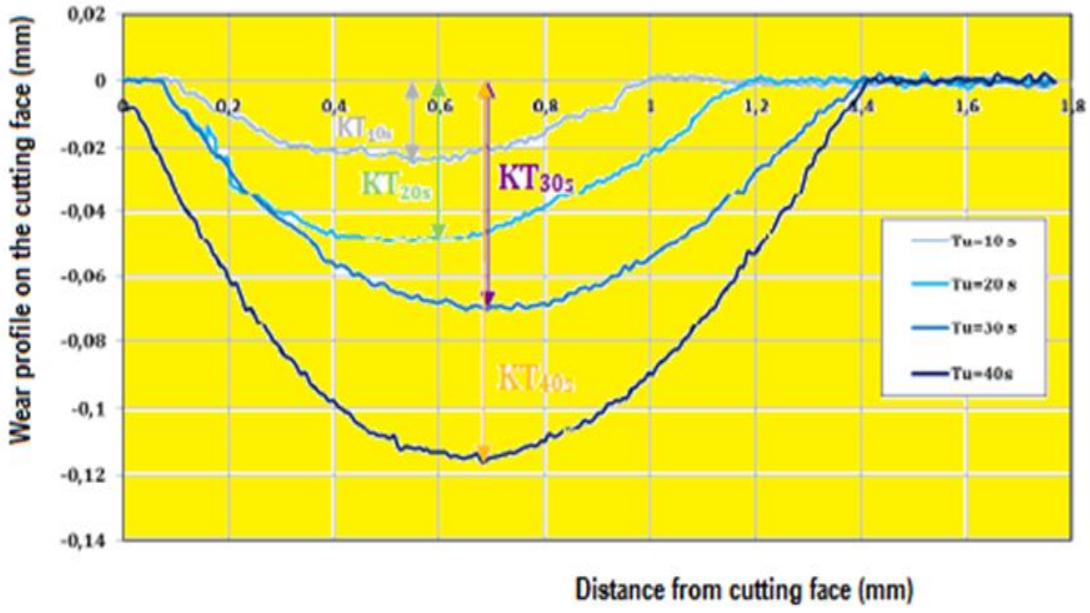

Figure 8: Evolution of crater wear over time for V_c = 150m/min; f = 0.2mm/rev; a_p = 3mm.

The evolution of crater wear over time as a function of the cutting parameters V_c and f is illustrated in Figure 9.

Volume 63 | Issue 02 | February 2024
DOI: 10.5281/zenodo.10682775

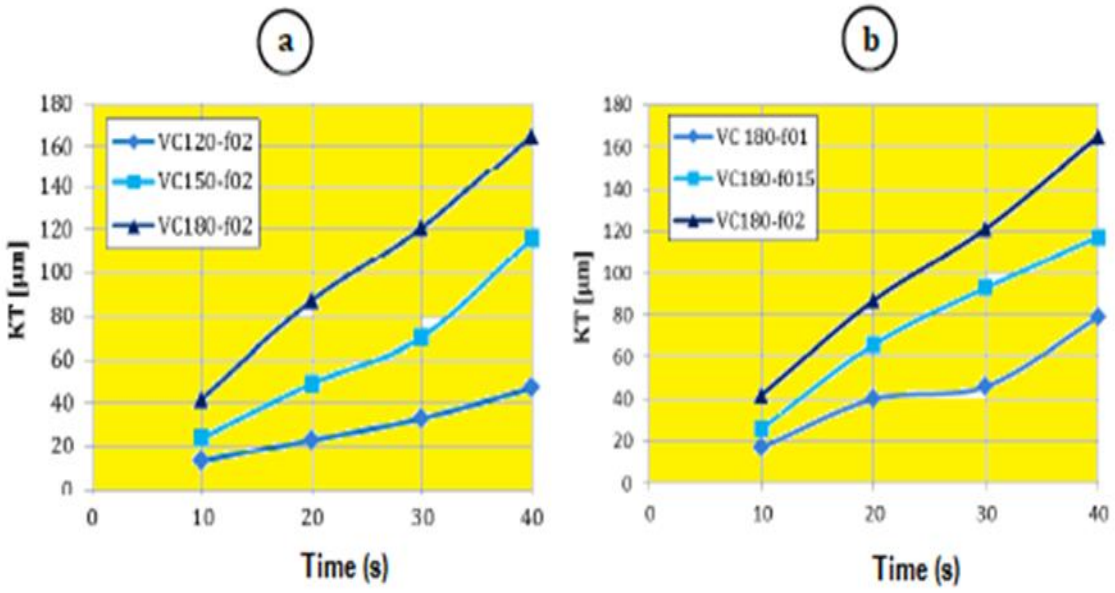

Figure 9: Evolution of KT crater wear over time: (a). depending on the cutting speed at constant feed: f=0.2mm/rev (b). depending on the feed at constant cutting speed: V_c=180m/min.

By analyzing Figure 9, we notice that the crater wear KT increases strongly with the cutting speed. This can be explained by the high temperatures, at the tool/chip interface, which occur for the highest cutting speeds and which promote wear by diffusion, among other things.

The crater wear KT also increases with the feed f given the increase in the volume of material to be removed. Unlike the KM and KT parameters measured on the rake face of the tool, flank wear VB is measured directly. Figure 10 illustrates the evolution of flank wear over time at 10s, 20s, 30s and 40s for the following cutting conditions: V_c=180m/min, f=0.2mm/rev and a_p=3mm.

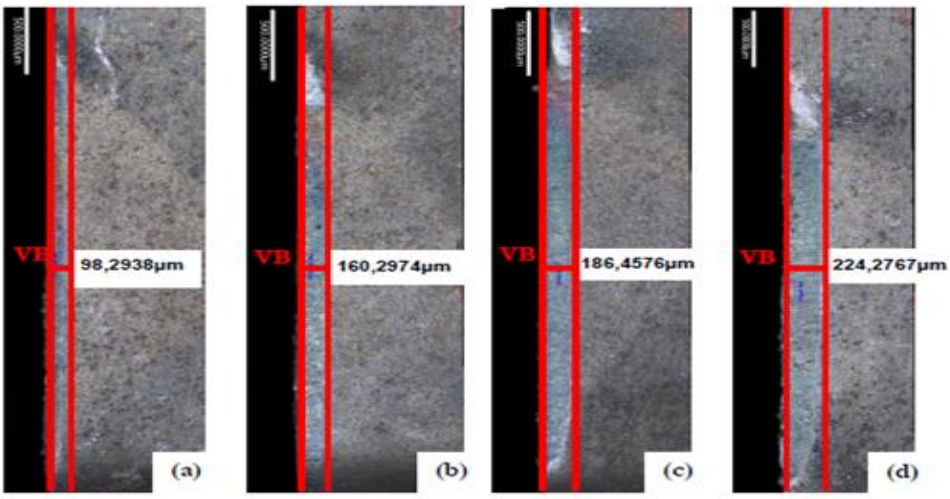

Figure 10: Evolution of flank wear over time: V_c = 180m/min; f = 0.1mm/rev; a_p = 3mm (a). T_u = 10s; (b). T_u = 20s; (vs). T_u = 30s; (d). T_u = 40s.

The evolution of flank wear over time as a function of the cutting parameters V_c and f is given in Figure 11.

Volume 63 | Issue 02 | February 2024
DOI: 10.5281/zenodo.10682775

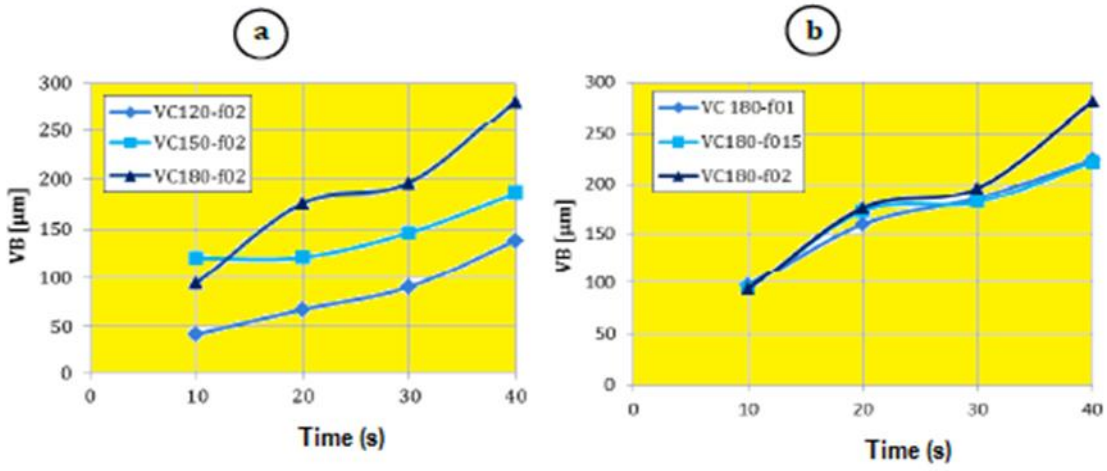

Figure 11: Evolution of flank wear VB over time: (a). depending on the cutting speed at constant feed: f=0.2mm/rev (b). depending on the feed at constant cutting speed: V_c=180m/min.

Figure 12 clearly shows that the flank wear VB is greater for the highest cutting speeds but it is also less sensitive to the increase in feed. For the measurement of the cutting and feed forces, the machining time is fixed at 40 seconds, only the cutting parameters V_c and f change: V_c = [120; 150; 180] m/min and f = [0.1; 0.2; 0.3] mm/rev. The evolution of the cutting forces and the feed forces over time is given respectively by Figure 10, and this for a cutting speed V_c = 120m/min, a feed f = 0.1mm/rev, a depth of pass $a_p = 3mm$ and a machining time T_u = 40s. Given that the machining forces are very unstable over time, a filtering function (moving average) was applied to obtain the average forces over time.

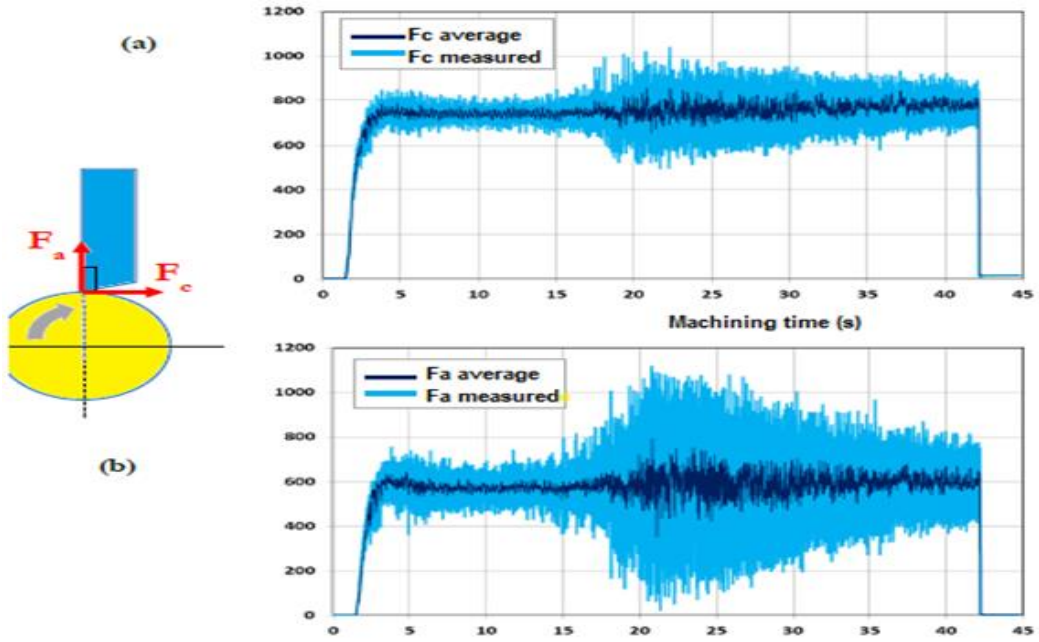

Figure 12: Machining forces for V_c = 120m/min; f = 0.1mm/rev; a_p = 3mm: (a). Cutting forces, (b). Efforts advance.

To better see the evolution of the cutting and feed forces, the average values for a different torque (V_c and f) after each test are grouped together in Table 2.

Volume 63 | Issue 02 | February 2024
DOI: 10.5281/zenodo.10682775

Table 2: Evolution of cutting and feed forces over time.

V_c = m/min	f = mm/rev	Fa average (N)	Fc average (N)
120	0,1	574	760
120	0,15	825	1173
120	0,2	984	1463
150	0,1	792	982
150	0,15	874	1190
150	0,2	893	1507
180	0,1	708	913
180	0,15	798	1164
180	0,2	820	1390

The Figures 13and 14, show the influence of the cutting parameters, in particular the cutting speed and the feed, on the evolution of the cutting and feed forces.

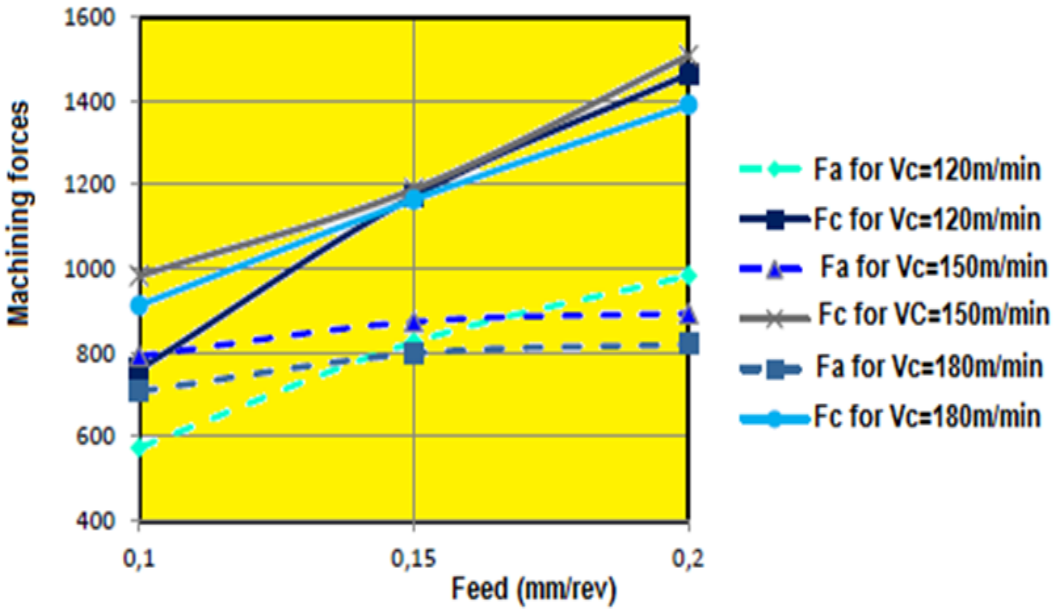

Figure 13: Evolution of the cutting and feed forces as a function of the feed f for different cutting speeds.

The first observation that can be seen from the curves in Figures 13 and 14 is that the cutting forces Fc are always higher than the feed forces Fa, regardless of the cutting parameters used. We can also say that the forces Fc increase strongly and almost linearly with the feed, whatever the cutting speed used. This is due to the fact that the volume of material to be removed is greater when the advance increases. Moreover, it is clearly noted that the advance forces Fa are less sensitive to the advance than the forces Fc but nevertheless increase when the advance increases. It should also be noted that the cutting forces vary slightly when the cutting speed increases. This evolution is almost stable. This evolution of the machining forces is found in the work of Moussaoui for the machining in orthogonal cut of the titanium alloy Ti6Al4V [40].

Volume 63 | Issue 02 | February 2024
DOI: 10.5281/zenodo.10682775

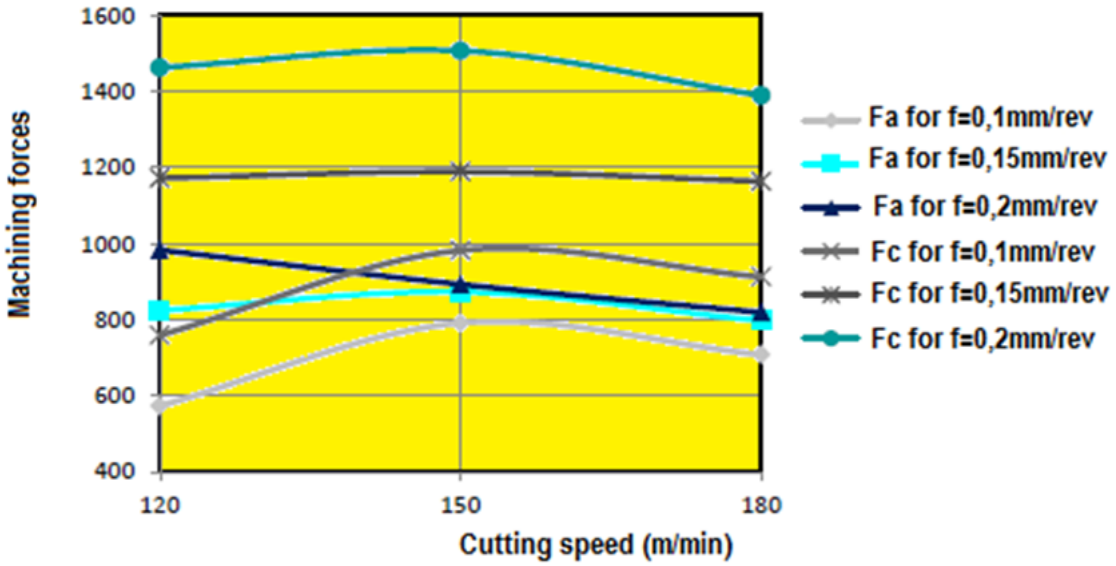

Figure 14: Evolution of the cutting and feed forces as a function of the cutting speed for different feeds.

Analysis of the experimental results reveals an almost linear evolution of the volume of wear over time, under the cutting conditions adopted: V_c= [120, 150, 180] m/min; f= [0 .1; 0.15; 0.2] mm/rev and T_u= [10, 20, 30, 40] s.

It therefore appears legitimate to opt for an 'Archard' type law for taking into account the wear phenomenon of the pad in the wear simulation. Once this steady state has been reached, it is therefore possible to apply Archard's law given by equation (1) on the nodes on the surface of the tool.

$$V = k\frac{F_n}{P_m}d \qquad (1)$$

Indeed this law is governed by the relation below which remains valid for the case of a sliding contact at constant speed [41].

V being the volume of worn material, k being the wear coefficient without units, F_n being the applied normal force, P_m being the flow stress of the softest material and d the distance covered.

Another form of Archard's law is adopted, it is equation (2) which gives the depth of wear h [mm] as a function of the distance traveled S [mm] and the contact pressure P [MPa].

$$h = \frac{k}{H}S.P \qquad (2)$$

k being the wear coefficient [without units] and H the hardness of the softest material [MPa]. For each node of the tool surface, the corresponding wear depth in the x direction is calculated.

The expression of the wear rate is therefore given by the following equation with Vg the sliding speed [m/s] and K=k/H the wear coefficient [MPa^{-1}].

Volume 63 | Issue 02 | February 2024
DOI: 10.5281/zenodo.10682775

$$\frac{h}{t} = K.V_g.P \qquad (3)$$

Wear will be taken into account by changing the coordinates of the tool according to equation (4).

$$\mathrm{X_{use}} = X_{unit} + \mathrm{h} \qquad (4)$$

The table 3 summarizes the numerical values of the depth of wear.

Table 3: Numerical values of wear depths for Vc = 120m/min; f = 0.1mm/rev and ap =3mm.

N node	P (MPa)	Vg (m/s)	T (s)	h (µm)	X init (mm)	X use (mm)
	326,57	2,2	11	0,228604	0,04341114	0,0363975
	4255,63	2,2	11	2,978933	0,04341114	0,0363975
	2378,32	2,2	11	1,664816	0,04341114	0,0363975

It should be remembered that the procedure for calculating the depth of wear and updating the geometry of the tool remains applicable as long as the depth of wear does not exceed the size of a mesh ($18\mu m$). Otherwise ($h > 18\mu m$), a purely elastic calculation is launched on ABAQUS/Implicit© [42] on a model containing the tool only. The latter will have as boundary conditions the displacements corresponding to the depths of wear.

Movements on nodes inside the tool are recovered. This will allow to have the new coordinates of the nodes even inside the tool. The distribution of the temperature fields in the cutting insert is given by the figure 15.

The new geometry of the tool, after 10 seconds of machining is presented in Figure 16.

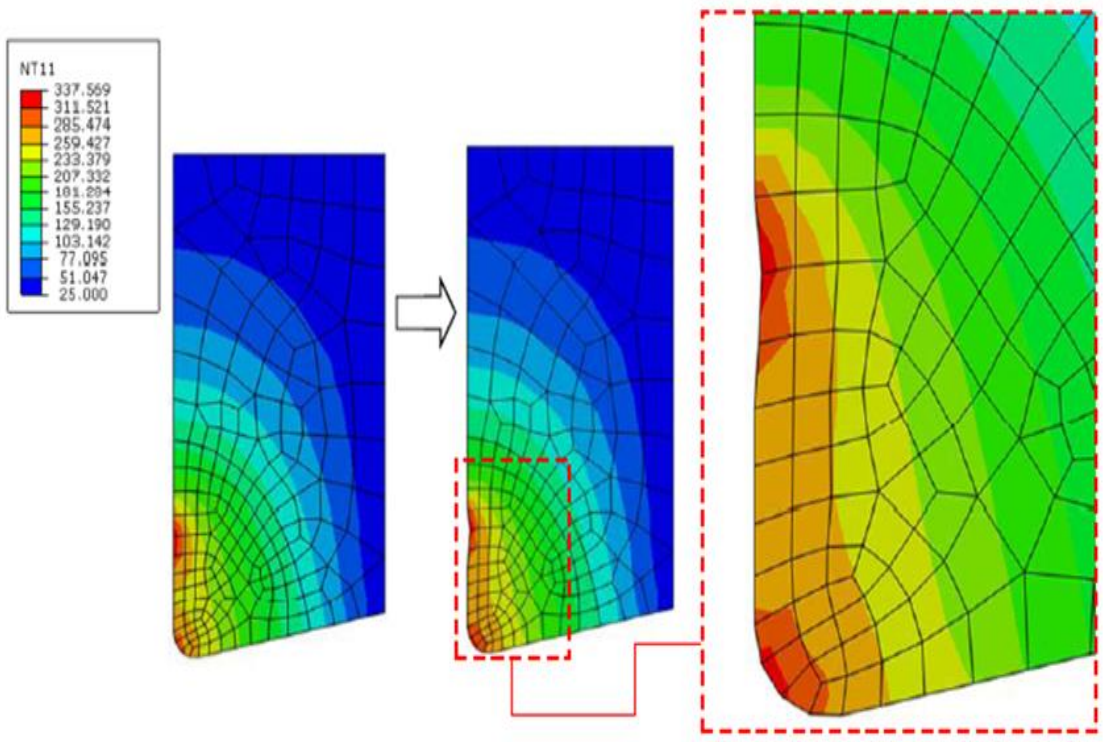

Figure 15: Temperature fields in the cutting insert and its geometry after the 1st wear calculation (state at 10 seconds of machining).

Volume 63 | Issue 02 | February 2024
DOI: 10.5281/zenodo.10682775

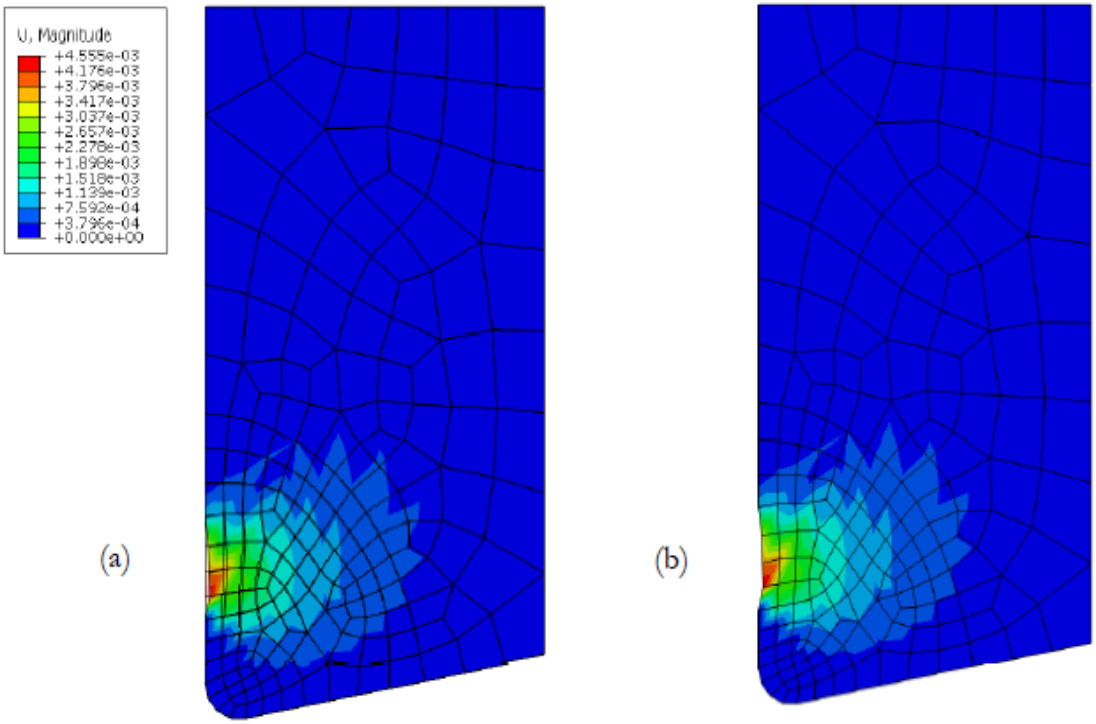

Figure 16: Update of the mesh after the calculation Implicit purely elastic (a). Initial and deformed mesh superimposed (b). Deformed mesh.

This figure show the strain generated by the wear of 42CrMo4 steel tool destined to the machining. The understanding of the wear mechanism of these tools lays a foundation for further research on the wear law of tools and for exploring the methods of prolonging the service life of tools [18].

4. CONCLUSION

The overall results can be summarized as follows:

- Our experimental study allowed us to investigate the wear of a cutting tool for the machining of 42CrMo4 steel. This study began with a test campaign to identify the range of speeds suitable for studying wear, namely 120, 150 and 180 m/min; the advances being equal to 0.1, 0.15 and 0.2mm/rev. Subsequently, 36 tests with different torques (V_c, f) were carried out to observe the wear phenomenon of the turning inserts for the different cutting conditions and also to follow its evolution over time.
- The wear appearing on the inserts following orthogonal cutting tests was observed by 3D microscopy. This made it possible to measure the wear parameters on the rake face of the tool (KM, KT and worn volume) and on the clearance face (VB). The influence of cutting parameters on the evolution of wear parameters was also studied.
- For each test, the machining forces (cutting forces and feed forces) were recovered, which made it possible to see their evolution as a function of the cutting speed and the feed.

Volume 63 | Issue 02 | February 2024
DOI: 10.5281/zenodo.10682775

- This research also made it possible to bring legitimacy to the choice of the application of Archard's law in the simulation of tool wear, given that the evolution of the volume of wear during time is almost linear under the mentioned cutting conditions and within a machining time interval of 40s.
- The analysis of the experimental results carried out revealed an almost linear evolution of the wear volume over time, under the cutting conditions adopted. It is therefore legitimate to opt for Archard's law to take into account the phenomenon of wear in the simulation of the cut.
- A model called “vertical” was chosen to increase the duration of simulated machining. It has been implemented in ABAQUS© using the PYTHON© programming tool.
- This procedure therefore facilitates the application of Archard's law to take into account the phenomenon of wear in the simulation of the cut. It is based on the relocation of the nodes of the surface of the tool after calculation of the depths of wear via Archard's law. The latter depends on the contact pressure and the sliding speeds on the surface of the tool and on a wear coefficient K.

Declaration of conflicting interests

The author(s) declared no potential conflicts of interest with respect to the research, authorship, and/or publication of this article.

References

1) A. S. Pyatykh, A. V. Savilov & S. A. Timofeev, Method of Tool Wear Control during Stainless Steel End Milling, Journal of Friction and Wear, volume 42, pages263–267 (2021). https://doi.org/10.3103/S1068366621040097
2) N. M. Rusin, A. L. Skorentsev & E. A. Kolubaev, Effect of Severe Plastic Deformation on Wear Resistance of Sintered Al–Sn Alloys under Dry Friction Against Steel, Journal of Friction and Wear volume 41, pages259–266 (2020). https://doi.org/10.3103/S1068366620030149.
3) V.Schulze, F.Bleicher, C.Courbon, M.Gerstenmeyer, L.Meier, J.Philipp, J.Rech, J.Schneider, E.Segebade, A.Steininger, K.Wegener, Determination of constitutive friction laws appropriate for simulation of cutting processes, CIRP Journal of Manufacturing Science and Technology, Volume 38, August 2022, Pages 139-158, https://doi.org/10.1016/j.cirpj.2022.04.008.
4) Andrea Cappella, Julien Vincent, Sylvain Philippon & Laurent Faure, High-Speed Contact Study between a Ti-6-Al-4V Tool and an Abradable Coating Using Ballistic Benches and a Dynamic Compensation Approach, Journal of Friction and Wear volume 38 (2017) 444–449. https://doi.org/10.3103/S1068366617060022
5) Fousseny KONÉ, Étude expérimentale, modélisation et simulation numérique de l’usinage à sec des aciers inoxydables : Étude de l’effet des revêtements mono et multi couches, Thèse Doctorat, Université De Lorraine (2012). http://www.culture.gouv.fr/culture/infos-pratiques/droits/protection.htm
6) Musfirah Abdul Hadi, Jaharah A. Ghani, Che Hassan Che Haron & Mohd. Shahir Kasim, Effect of cutting speed on the carbide cutting tool in milling Inconel 718 alloy. Journal of Materials Research volume 31 (2016), pages1885–1892

Volume 63 | Issue 02 | February 2024
DOI: 10.5281/zenodo.10682775

7) Barge M, Hamdi H, et al, Numerical modelling of orthogonal cutting: influence of numerical parameters. Journal of Materials Processing Technology, 164-165 (2005): 1148-1153.

8) Jinxuan Bai, Qingshun Bai, Zhen Tong, Guoda Chen, The influence of cutting parameters on the defect structure of subsurface in orthogonal cutting of titanium alloy. Journal of Materials Research, 33 (2018) , pages720–732

9) Changchun Lv, Xiaoyong Ren, Chengbiao Wang & Zhijian Peng, Improved mechanical performance and wear resistance of Ti-coated cBN–WC–Ni composites. Journal of Materials Research volume 34 (2019) , pages3844–3852

10) Mabrouki T, Girardin F et al, Numerical experimental study of dry cutting for an aeronautic aluminium alloy (A2024-T351), International Journal of Machine Tools and Manufacture, 48 (11) (2008), 1187-1197.

11) B. N. Fedulov, D. A. Bondarchuk, A. N. Fedorenko & E. V. Lomakin, Residual stresses near the free edge of composite materials, Acta Mechanica volume 233 (2022) , pages417–435

12) Bibeye Jahaziel Ronadson, Krishnaraj Vijayan, Sudhagar Sanmugam, Geetha Priyadarshini Badhirappan, Improving dry machining performance of surface modified cutting tools through combined effect of texture and TiN-WS2 coating, Journal of Manufacturing Processes, Volume 85 (2023) , Pages 101-108.

13) Jinhua Wang a 1, Jie Zhang a 1, Ruitao Peng b, Xianggang Zhao a, Guolong Zhao a, Ni Chen a, Liang Li c, Ning He a, Xiuqing Hao, Research on cutting parameters of low-temperature liquid CO2 assisted PCD tool turning bearing ring, Journal of Manufacturing Processes, Volume 87 (2023), Pages 199-208

14) Renzhe Chen, Coby Turman, Mingliang Jiang, Negar Kalantar, Michael Moreno & Anastasia Muliana Mechanics of kerf patterns for creating freeform structures, Acta Mechanica volume 231 (2020), pages3499–3524

15) C. Spitas, V. Spitas, A. Amani & M. Rajabalinejad, Parametric investigation of the combined effect of whole depth and cutter tip radius on the bending strength of 20° involute gear teeth, Acta Mechanica volume 225 (2014) 361–371

16) S. Tsutsumi, R. Fincato & H. Momii, Effect of tangential plasticity on structural response under non-proportional cyclic loading, Acta Mechanica volume 230 (2019) 2425–2446

17) S. Abolfazl Zahedi, Anish Roy & Vadim V. Silberschmidt, Variation of cutting forces in machining of f.c.c. single crystals, Acta Mechanica volume 227 (2016) 3–9

18) Gökhan Sur a, Ali Riza Motorcu b, Samet Nohutçu, Single and multi-objective optimization for cutting force and surface roughness in peripheral milling of Ti6Al4V using fixed and variable helix angle tools, Journal of Manufacturing Processes, Volume 80 (2022) 529-545.

19) Courbon C, Vers une modélisation physique de la coupe des aciers spéciaux : intégration du comportement métallurgique et des phénomènes tribologiques et thermiques aux interfaces. Thesis supported by the Centrale School of Lyon (2011).

Volume 63 | Issue 02 | February 2024
DOI: 10.5281/zenodo.10682775

20) Jaharah A. Ghani, Che Hassan Che Haron, Mohd Shahir Kasim, Mohd Amri Sulaiman & Siti Haryani Tomadi, Wear mechanism of coated and uncoated carbide cutting tool in machining process. 31 (2016) 1873–1879

21) Jinxuan Bai, Qingshun Bai, Zhen Tong, Chao Hu & Xin He, Evolution of surface grain structure and mechanical properties in orthogonal cutting of titanium alloy Journal of Materials Research volume 31 (2016) 3919–3929

22) Saadlaoui Y, Modélisation des conditions de contact outil-copeau en coupe orthogonale, Master 2 Research Dissertation, National School of Engineering of Saint-Etienne (2017).

23) Bing Liu, Haijie Yang, Ruijie Kong, Xinyu Wang, Jiaqi Liu, Kuo Pang, Simulation and experimental study on limited cutting and heat effect of silicon carbide Materials Today Communications, Volume 33 (2022) 104378, https://doi.org/10.1016/j.mtcomm.2022.104378

24) Hashemi J, Tseng AA et al, Finite element Modelling of segmental chip formation in high-speed machining, Journal of Material Engineering and Performance, 3(5) (1994) 712-721.

25) Bäker M, Finite element simulation of high-speed cutting forces, Journal of Materials Processing Technology, 176 (2006) 117-126.

26) Ning Yang, Xin Yang, Wen Huang, Shun Zhao, Dajiang Lei, Analysis of diamond tool wear mechanism in terms of stress for KDP Fly cutting, Materials Today Communications, Volume 30 (2022) 103146, https://doi.org/10.1016/j.mtcomm.2022.103146.

27) L. Zouambi, M. Bourdim, et all. Determination of a Mathematical Model of Taper Wear for a Longitudinal Surfacing Operation. International Journal Of Energy And Environment. Vol 16, (2022). DOI: 10.46300/91012.2022.16.10.

28) Shaw, M.C. Metal cutting principles, NY: Oxford University Press (2005).

29) Khrais SK and Lin YJ, Wear mechanisms and tool performance of TiAlN PVD coated inserts during machining of AISI 4140 steel, Wear, 262 (1- 2) (2007) 64-69.

30) Yen Y, Söhner J et al, Estimation of tool wear in orthogonal cutting using the finite element analysis, Journal of Materials Processing Technology, 146 (2004) 82-91.

31) Xie LJ, Schmidt J et al, 2D FEM estimate of tool wear in turning operation, Wear, 258 (10) (2005) 1479-1490.

32) M. Bourdim, L. Zouambi, M. Djilali Beida, S. Kerrouz, Determination of a wear law for uncoated cutting tools, International Journal of Systems Applications, Engineering & Development, Volume 16, (2022), DOI: 10.46300/91015.2022.16.12.

33) Anibal Faruk Abedrabbo, Juan Camilo Osorio, Sepideh Abolghasem, Carlos Valencia, Fabio Rojas, Predicting subgrain size and dislocation density in machining-induced surface microstructure of nickel using supervised model-based learning, Materials Today Communications, Volume 30 (2022) 103162, https://doi.org/10.1016/j.mtcomm.2022.103162.

Volume 63 | Issue 02 | February 2024
DOI: 10.5281/zenodo.10682775

34) Shivaprakash Y M,Gurumurthy BM, Jamaluddin Hindi, Muralishwara K & Sathyashankara Sharma, Investigation on the effect of machining parameters on 42CrMo4 DPS steels. Cogent Engineering. Vol 10, Issue 1, (2023). https://doi.org/10.1080/23311916.2022.2162954.

35) Marek Madajewski, Zbigniew Nowakowski, Finite Element Analysis Of Influence Of Flank Wear Evolution On Forces In Orthogonal Cutting Of 42CrMo4 Steel, Archives of Mechanical Technology, Vol. 37, 58-64, (2017). DOI: 10.1515/amtm-2017-0009.

36) Mokhtar Bourdim, Leila Zouambi, Siham Kerrouz, Wahid Oudad, Contribution To The Study Of The Influence Of Cutting Temperature In Hard Turning, Acta Technica Napocensis, Vol. 65, Issue I, 2022, https://atna-mam.utcluj.ro/index.php/Acta/article/view/1776.

37) Marinov V, Experimental study on the abrasive wear in metal cutting, Wear, 197 (1996) 242-247.

38) Jiyun Kong, Yuanyuan Tian, Xin Zeng, Bin Liu, Qihong Fang & Jia Li, Friction and wear behavior of a precipitation-hardened equiatomic FeCrNi medium entropy alloy unraveled by molecular dynamics simulation. Journal of Materials Research volume 37 (2022) 3009–3020

39) Moussaoui K, Influence de l'usinage sur la durée de vie en fatigue de pièces aéronautiques en alliage de titane. Thesis supported by the University of Toulouse III Paul Sabatier (2013).

40) Archard JF, Contact and Rubbing of Flat Surfaces, Journal of Applied Physics, 24 (8) (1953) 981-988.

41) Abaqus/CAE Ver 6.11, User's Manual, Hibbitt, Karlsson & Sorensen, Inc, (2011).